International Journal of Heat and Technology
Vol. 40, No. 4, August, 2022, pp. 917-926
Journal homepage: http://iieta.org/journals/ijht

Entropy Generation of Graphene Nanoplatelets in Micro and Mini Channels: Nanofluid Flow in Automotive Cooling Applications

Luke O. Ajuka[1], Omolayo M. Ikumapayi[2,4*], Esther T. Akinlabi[3]

[1] Department of Automotive Engineering, University of Ibadan, Ibadan 200005, Nigeria
[2] Department of Mechanical and Mechatronics Engineering, Afe Babalola University, Ado Ekiti 360101, Nigeria
[3] Department of Mechanical and Construction Engineering, Northumbria University, Newcastle, NE7 7XA, United Kingdom
[4] Department of Mechanical and Industrial Engineering Technology, University of Johannesburg, DFC, Johannesburg 2092, South Africa

Corresponding Author Email: ikumapayi.omolayo@abuad.edu.ng

https://doi.org/10.18280/ijht.400408

Received: 12 June 2022
Accepted: 16 August 2022

Keywords:
graphene nanoplatelet, nanofluid, laminar flow, entropy generation, mini-channel, microchannel

ABSTRACT

The present study examines the entropy generation of graphene nanoplatelet (GnP) suspended in different basefluids, theoretically. GnP in water (W), ethylene glycol (EG) and ethylene glycol- water (EGW, 1:1) was examined under laminar flow state in a unit length mini and micro-channel of 3mm and 0.05mm diameter. The coefficient of conductivity (C_k) and viscosity ($C\mu$) of the nanofluid were determined from experimental analysis and their order of magnitude were established for analysis of entropy generation in mini and micro-channels. Entropy generation by fluid friction (Ṡgen, ff) in the channels containing EG was higher than with W and EGW by 75.6% and 79.9%, respectively. Thermal irreversibility (Ṡgen, th) of W was lower by132.9% and 58.2% compared to EG and EGW. Sgen,th in all the fluids decreased with increased solid volume fraction in mini-channels, while, Ṡgen,ff increased with increase in volume fraction for micro-channels. Total entropy generation (Ṡgen, tot) of water was lower by 75.6% and higher by 64.8% compared to EG and EGW, respectively in a micro-channel, whereas Ṡgen, tot of water was lower by 123.7% and 38.4% compared to EG and EGW, respectively. As GnP volume fraction was increased in the basefluids, entropy generation ratio decreased, highlighting the positive influence of thermal properties of the nanofluid. A lower Bejan number for water (Be_w), 36.8% and 358.9% were observed compared to EG and EGW in micro-channel, whereas Be_w was lower by 3.8% and 13.8% when compared to EG and EGW nanofluids in the mini channel.

1. INTRODUCTION

The novel approach of using heat transfer fluids (HTF) in thermal management to enhance energy savings is gaining enormous attention as energy consumption keeps increasing across the globe. Sustainability in the direction of reliable energy efficiency and enhancement at all levels has been reported to have declined [1]. Quality energy loss and reduction in the efficiency, reliability and expected life of systems due to heat generated especially in the more compact electronic devices with high densities of chips could be addressed by enhancing their heat transfer capabilities aside working with optimum geometry. It has been reported in literatures that the conventional heat transfer fluids (HTFs), e.g., water, ethylene glycol, mineral oil, transformer oil, etc., possess a less than unity thermal conductivities (K), which makes them to remain a limitation in efficient thermal management, but an increase in HTFs thermal conductivity will lead to an increase in solids-HTFs conductive heat flux based on Fourier's law ($\boldsymbol{jQ} = -k\boldsymbol{\nabla}T$). Nanoparticle dispersion has become a unique method for thermal property enhancement by blending them with base-fluids in thermodynamic cycles. Several findings have established nanofluids to possess not only higher thermal conductivity than the host fluids., but to generate an enhanced frictional pressure drop. Meanwhile, nanotechnology has become one of the emerging researchable solutions in heat pipes, sensors, micro/mini channels, clean energy devices, heat sinks, composite materials, automobiles, medicine, cosmetic, air-conditioning and refrigeration, solar energy device, lubricants, and coolants applications through the suspension of ultrafine nano-dimensioned (<100 nm) solid particles to enhance the thermo-physical characteristic of the base fluid matrix [2-4]. The challenges with micrometer-dimensioned solid particles includes abrasion, sedimentation, and the risk of clogging, whereas the unique quality of nanofluids for various desirable utilization includes its excellent heat conductivity, heat transfer capability, stability, friction coefficient, erosion reduction and lubrication. While nanoparticles are prepared in tubular (single or multi-walled carbon nanotubes); spherical (metals, metallic oxides, etc.) and layered (graphene, graphene nanoplatelets) forms [5-12].

Carbon nanotubes have remained the most researched carbon-related nanomaterials in applications involving nanofluids [13-18], recently however, report by Balandin et al. [19] that graphene showed better thermal conductivity compared to carbon nanotubes, is repositioning research focus on the thermo-physical properties of different graphene based

nanofluids [20-25]. Graphene is a carbon-like, graphite monolayer with reported excellent carrier mobility [26], transport performances [27], high specific surface area [28], Young's modulus [29] and thermal conductivities in ranged between 2000 Wm K to 5350 WmK [19, 30, 31], making the allotrope an excellent choice for heat transfer applications. The convective heat transfer of graphene nanoplatelets (GNP) nanofluids depends primarily on the thermal conductivity and the viscosity of the nanofluid. Such Graphene based studies include the investigation carried-out by Monireh et al. [32] which investigated the effect of nano-sheets mass fraction on the thermal-properties of glycerol and multilayered-graphene nanofluids. They reported that there was an increase in viscosity as solid mass fraction within 0.0025 to 0.0200 is increased, with emphasis on a viscosity enhancement of 401.49% for 2% graphene nano-sheets fraction added at a shear rate of 6.32 s1 and 20℃, respectively [32]. Selvam et al. [33] carried out a thermal conductivity improvement study on ethylene glycol and water using graphene nanoplatelets and sodium deoxycholate as surfactant. They reported that using a transient hot wire (THW) method, the recorded enhancement for a 0.5 vol% loading of graphene nanoplatelets doped in ethylene glycol and water were approximately 21% and 16%, respectively. They noted that interfacial thermal resistance between graphene nanoparticle and the ethylene glycol and water affects the thermal conductivity significantly, giving 2.2 × 10−8m^2 KW^{-1} and 1.5 × 10−8m^2 KW^{-1} values, respectively [33]. Esfahani et al. [34] conducted an experimental study on the heat transfer and pressure drop of synthesized Graphene Oxide nanofluids using the modified Hummers method. They examined three heat flux conditions of 7.4, 9.1, and 12.6 kW/m^2. They noted that at constant pump frequency, there was a decrease in flowrate and Reynolds number from 0.01 wt.% to 0.1 wt.% of graphene oxide due to an increase in viscosity. Having formulated correlations for Nusselt number and Reynolds number from literature using multiple regression analysis, they reported that at 0.01 wt.% of graphene oxide, the convective heat transfer coefficient was higher than 0.1 wt.% of graphene oxide and water. They concluded that Nusselt number was insignificant with the heat flux and velocity variation [34]. Bahaya et al. [35] carried out a thermal conductivity test and its effect on increased viscosity using graphene nanoplatelets (GNP). They reported a maximum thermal conductivity enhancement ratio of 1.43 at a volume fraction of 0.014 using water as base-fluid. They noted that there was good agreement between the experimental measurement and the Einstein model with an adjustment factor of 2151 intrinsic viscosity. They concluded that there is a decrease in heat transfer in laminar section for external flows using GNP nanofluids compared to water [35].

For engineering systems, an increase in heat transfer does not particularly indicate a drop in irreversibility (fluid friction, fluid mix for laminar or turbulence, non-quasi-static compression or expansion, chemical reactions, thermal heat flow) which leads to increased system entropy generation, particularly when assessing heat exchanger effectiveness [36, 37], but by evaluating the entropy generations caused by finite temperature gradient within such system [38-40]. Bejan [41] established that the entropy generation consists of two parts namely, (i) irreversibility associated with frictional factors (ii) thermal irreversibility [41, 42]. Although there are speculations of enhanced thermal conductivity which have been reported about Graphene nanoplatelets (GNPs) owing to its 5 to 10 nm thickness quality crystals, two-dimensional make-up and room temperature ballistic transport [43-45], it is vital to show the entropy generation of this nanoparticle in various basefluids due to extensive application potential.

There are no explicit studies in literature for entropy generation of GNP nanofluids in different basefluids, hence, this study aims to analyze the entropy generation in heat conducting Graphene nanoplatelets (GNPs) nanofluids within micro and minichannels (Figure 1) under laminar flow regimes using different basefluids.

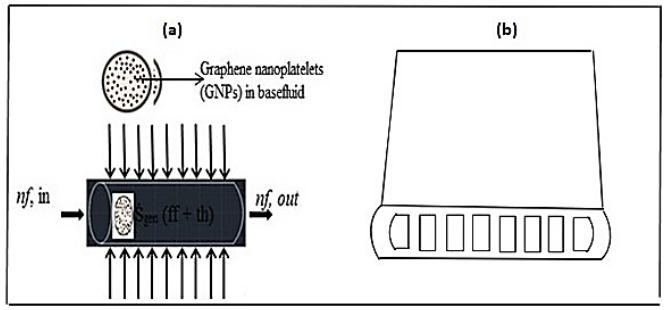

Figure 1. Schematic representation of micro/mini channel illustrating (a) Entropy generation as nanofluid flows through; (b) Electronic multiport channel

2. METHODOLOGY

In a heat conducting duct of known diameter (D), the fundamental entropy governing equations as stated by Bejan [41, 42] based on entropy generation rate are presented in Eqns. (1) and (2):

$$\dot{S}GEN = (\dot{S}GEN)_{ff} + (\dot{S}GEN)_{th} \quad (1)$$

where, $\dot{S}GEN_{, ff}$ and $\dot{S}GEN_{, th}$ are the irreversibilities due to fluid friction and thermal heat, respectively.

$$\dot{S}GEN = \frac{8m^3}{T\rho^2\pi^2}\frac{f((Re)_D)}{D^5} + \frac{D^2\pi q''^2}{T^2 kNu\left((Re)D,\ Pr\right)} \quad (2)$$

where, Reynold's number (Re) =4m/πμD; frictional factor (*f*) = 64/Re.

The two parts of the Eq. (2) comprise the entropy generation as a result of frictional characteristic and as a result of heat transfer (transport). The first part is a function of mass flow rate (ṁ), density (ρ), Reynolds number (Re) and duct diameter (D), while the Nusselt number, heat flux and Prandtl number are highly significant in the second part. A small hydraulic diameter was assumed with a constant Nusselt number (48/11) in the fully developed laminar flow, independent of axial position, Reynolds and prandtl numbers.

Consider heat transfer under hydrodynamically and thermally developed flow (Figure 1) with uniform wall heat flux condition is given by;

Governing equation;

$$u\frac{\partial T}{\partial x} + v\frac{\partial T}{\partial r} = \frac{\propto}{r}\frac{\partial}{\partial r}\left(r\frac{\partial T}{\partial r}\right) \quad (3)$$

where, x and y are velocities in different directions. Under hydrodynamically fully developed conditions; $v = 0, \frac{\partial u}{\partial x} = 0\ and\ u(r) = 2u_m\left[1 - \left(\frac{r}{r_0}\right)^2\right]$, so, eqn. 1 can be re-written as;

$$2u\left[1-\left(\frac{r}{r_0}\right)^2\right]\frac{dT_m}{dx}=\frac{\propto}{r}\frac{\partial}{\partial r}\left(r\frac{\partial T}{\partial r}\right) \quad (4)$$

For any point x of the particle, $\frac{dT}{dx}=\frac{dT_m}{dx}$; solving for T at any x (r), T becomes a function of r (where $dT_m/d\,x$), T becomes a function of r only. Hence,

$$\frac{1}{r}\frac{d}{dr}\left[r\frac{dT}{dr}\right]=\frac{2u_m}{\propto}\frac{dT_m}{dx}\left[1-\left(\frac{r}{r_0}\right)^2\right] \quad (5)$$

Multi-step integral of Eq. (3) can be re-written as;

$$T(r)=\frac{2u_m}{\propto}\frac{dT_m}{dx}\left[\frac{r}{4}-\frac{r^4}{16r_0^2}\right]+C_1 Inr+C_2 \quad (6)$$

At r = 0, T is finite; $C_1 = 0$, at r = r_0, T= T_w;

$$C_2=T_w-\frac{2u_m}{\propto}\left(\frac{dT_m}{dx}\right)\frac{3r_0^2}{16}$$

Hence, $T(r)=T_w-\frac{2u_m}{\propto}\frac{dT_m}{dx}\left[\frac{3}{16}+\frac{1}{16}\left(\frac{r}{r_0}\right)^4-\frac{1}{4}\left(\frac{r}{r_0}\right)^2\right]$.

So, $T_m=\frac{2}{u_m r_0^2}\int_0^{r_0}u(r)T(r)rdr = \int_0^{r_0}u(r)T(r)rdr/\int_0^{r_0}u(r)rdr$.

$$T_m=\frac{\int_0^{r_0}2u_m\left(1-\frac{r^2}{r_0^2}\right)r\left[T_w+\frac{q_w^{"}r_0}{k}\left\{\left(\frac{r}{r_0}\right)^2-\frac{1}{4}\left(\frac{r}{r_0}\right)^4-\frac{3}{4}\right\}\right]dr}{\int_0^{r_0}2u_m\left[1-\left(\frac{r}{r_0}\right)^2\right]rdr} \quad (7)$$

$$T_m=\frac{2u_m\left[T_w\left(\frac{r_0^2}{2}-\frac{r_0^4}{4r_0^2}\right)+\frac{q_w^{"}r_0}{k}\int_0^{r_0}\left(r-\frac{r^3}{r_0^2}\right)\left(\frac{r^2}{r_0^2}-\frac{1}{4}\frac{r^4}{r_0^4}-\frac{3}{4}\right)\right]dr}{2u_m\left[\frac{r_0^2}{2}-\frac{r_0^4}{4r_0^2}\right]}$$

$$T_m-T_w=\frac{q_w^{"}r_0}{k}\left(-\frac{11}{24}\right)$$

$$\frac{q_w^{"}}{(T_m-T_w)}\frac{2r_0}{k_f}=Nu_D=\frac{2\times24}{11}=\frac{48}{11}=4.36$$

(independent of Reynold and Prandtl numbers)

where, $q_w^{"}=h(T_w-T_m)=k_f\frac{dT}{dr}|r=r_0$, Nu_D = Nusselt number, Tw = wall temperature, Tm = mean temperature, q" = heat flux.

The irreversibility due to fluid friction, ṠGEN can be rewritten as depicted in Eq. (8).

$$\dot{S}GEN=\frac{128m^2\mu}{T\rho^2\pi D^4}+\frac{D^2\pi q^{"2}}{4.365\,KT^2} \quad (8)$$

Let $\Delta_1=\frac{128\,m^2}{D^4\,\pi}$ and $\Delta_2=\frac{D^2\pi q^{"2}}{4.365}$.

Hence, by rewriting ṠGEN in Eq. (8), we have, Eq. (9).

$$\dot{S}GEN=\frac{\Delta_1\mu}{T\rho^2}+\frac{\Delta_2}{kT^2} \quad (9)$$

The ratio of nanofluid to basefluid entropy generation is given by Eq. (5);

$$\frac{\dot{S}_{GENbf}}{\dot{S}_{GENnf}}=\left(\frac{K_{nf}}{K_{nf}}\right)\left(\frac{T_{bf}}{T_{nf}}\right)^2\left(\frac{\rho_{bf}}{\rho_{nf}}\right)^2\left(\frac{\Delta_{2\,nf}\rho^2{}_{nf}+\Delta_{1,nf}\mu_{nf}T_{nf}\;K_{nf}}{\Delta_{2\,bf}\rho^2{}_{bf}+\Delta_{1,bf}\mu_{bf}T_{nf}\;K_{bf}}\right) \quad (10)$$

Irreversibility is influenced by entropy generation, for example, low Irreversibility and entropy leads to better efficiency, hence, rate of entropy generation in nanofluid should be lower than the basefluid'. Therefore, ṠGEN, $_{nf}$ / ṠGEN, $_{bf}$ < 1 [46].

2.1 Thermophysical properties of nanofluid

The thermophysical properties of the nanofluid like density, viscosity, thermal conductivity and specific heat capacity should be supplied in the relating equations, as they are reported to contribute significantly to the nanofluid heat transfer process.

From the Hamilton-Cross proposed thermal conductivity equation as presented in Eq. (11) [47];

$$Ke=\frac{K_{bf}\left[K_p+(n-1)K_{bf}-(n-1)\emptyset(K_{bf}-K_p)\right]}{\left[K_p+(n-1)K_{bf}+(K_{bf}-K_p)\emptyset\right]} \quad (11)$$

where, the empirical shape factor n = 3/Ψ; and is 1 (unity), because Ψ=3 for spherical shape. Ke is the effective thermal conductivity, Kbf and Kp are the basefluid and nanoparticle thermal conductivities.

Eq. (11) representing the Hamilton-Cross thermal conductivity equation reduces for spherical nanoparticles to Eq. (12) [48];

$$Ke=K_{bf}(1+3\emptyset) \quad (12)$$

Thermal conductivity and viscosity of the nanofluid can be obtained as presented in Eqns. (13) and (14) respectively;

$$K_{nf}=K_{bf}(1+C_k\emptyset) \quad (13)$$

$$\mu_{nf}=\mu_{bf}(1+C_\mu\emptyset) \quad (14)$$

where, C_k and C_μ are conductivity and viscosity coefficients. A plot of the relative conductivities and viscosities of graphene-based nanofluids from literature data are given in Figures 2 and 3.

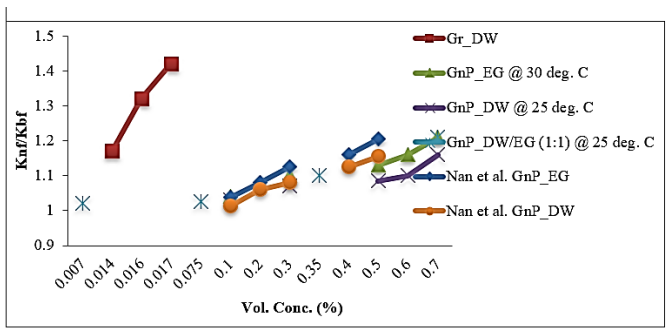

Figure 2. Relative conductivity variation of graphene-based nanofluids with volume fraction [33, 49-52]

Figures 2 and 3 show the variation in thermal conductivity ratio and viscosity ratio to determine the values of C_k and Cμ,

using a linear fit, the obtained values were 3.5 and 11, respectively. Linearized effective thermal conductivity of nanofluids is given as; $\frac{k_{nf}}{k_{bf}} = 1 + C_k\emptyset + 0(\emptyset^2)$; where $C_k = 3$ according to Maxwell. These values (C_k and C_μ) obtained, were also within acceptable set limits based on Hamilton-Cross equation and Prasher effective thermal condition for nanofluids (C_μ/C_k <4) [53]. Specific heat of nanofluid can be evaluated as using Eqns. (15) and (16):

$$Cp_{nf} = \frac{Cp_{bf}\rho_{bf}(1-\emptyset) + \rho_p\emptyset Cp_p}{\rho_{bf}(1-\emptyset) + \rho_p\emptyset} \quad (15)$$

The total density of the nanofluid is determined by:

$$\rho_{nf} = \rho_{bf}(1-\emptyset) + \rho_p\emptyset \quad (16)$$

In this study, entropy generation ratio is simplified. Eq. (11) is developed by parametric approximation, hence, the approximate Bejan equation is applied to analyze the heat transfer in micro and mini channels under laminar condition for different basefluids.

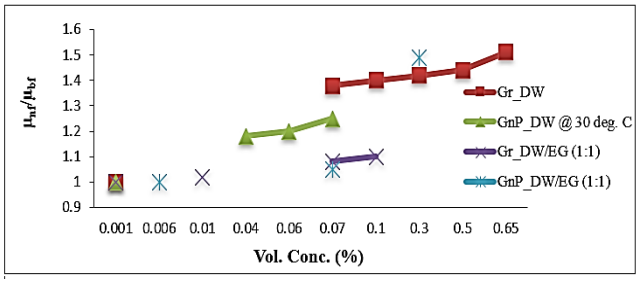

Figure 3. Relative viscosity variation of graphene-based nanofluids with volume fraction [33, 49-52]

2.2 Parametric order in microchannels

Entropy generation ratio for the micro-channel (d = 0.05mm) illustrated in Figure 1 is evaluated using Eq. (5) with the following parametric values of temperature (T) α 10^2, thermal conductivity (K) α1, mass flowrate (ṁ) ∝ 10^{-4}, Heat flux (q") α 10^2, viscosity (μ) α 10^{-3}, diameter (D) α 10^{-4}, density (ρ) α 10^3, indicating that $\Delta_1\mu KT$ α 10^9, $\Delta_2\rho^2$ α10^6, and $\Delta_2\rho 2$ are negligible compared to $\Delta_1\mu KT$. Therefore, Eqns. (17) and (18) are developed.

$$\frac{\dot{S}_{gen,nf}}{\dot{S}_{gen,nf}} = \left(\frac{T_{bf}}{T_{nf}}\right)\left(\frac{\mu_{nf}}{\mu_{bf}}\right)\left(\frac{\rho_{bf}^2}{\rho_{nf}^2}\right) \quad (17)$$

Assuming homogenous fluid state, $T_{nf} \approx T_{bf}$, and substituting Eqns. (14) and (16) into (17) gives therefore, the ratio

$$\frac{\dot{S}_{gen,nf}}{\dot{S}_{gen,bf}} = \left(\frac{\mu_{nf}}{\mu_{bf}}\right)\left(\frac{\rho_{nf}^2}{\rho_{bf}^2}\right) \cong \frac{1+11\emptyset}{1+\left(\frac{\rho_p}{\rho_{bf}}-1\right)\emptyset} \quad (18)$$

The ratio obtained in Eq. (18) is always positive and greater than unity since the density ratio ρ_p/ρ_{bf} is always greater than 1 (refer Table 1). As a result, it is not suggested to employ nanofluids in microchannels with laminar flow.

$$Be = \frac{\dot{S}_{genΔT}}{\dot{S}_{genΔP} + \dot{S}_{genΔT}} = \frac{1}{1+\emptyset} \quad (19)$$

Since $\dot{S}_{genΔP} = (1+\emptyset)\dot{S}_{gen,ΔT}$

where: $\dot{S}_{genΔT}$ = entropy generated by heat transfer irreversibility; $\dot{S}_{genΔP}$ = entropy generated by fluid friction irreversibility

2.3 Parametric order in mini-channels

For a mini-channel (3 mm diameter) under laminar regime, evaluating with Eq. (5) at temperature (T) α 10^2, thermal conductivity (K) α1, mass flow-rate (ṁ) ∝ 10^{-3}, viscosity (μ) α 10^{-3}, Heat flux (q") α 10^4, diameter (D) α 10^{-3}, density (ρ) α 10^3, values of $\Delta_2\rho^2 \propto 10^8$ and $\Delta_1\mu KT \propto 10^7$ determined are comparable for a mini-channel laminar flow, implying the influence of the aforementioned variables on entropy generation based on operation condition for this case. This implies that nanofluid effectiveness can be examined for various applications using heat transfer equation for analysis. Hence, this is applied to determine the entropy generation in mini-channels with the under-listed properties and flow condition in the Table 1.

Table 1. Thermophysical properties of base fluids and nanoparticle [52, 54-58]

	Basefluids			Nanoparticle	
Parameters	**DW**	**EG**	**DW-EG**	**GnP**	**Others**
Length of channel (m)					1
Conductivity of Base fluid	0.601	0.258	0.380	3000	
Viscosity (mPa_s)	0.891	0.00209	0.000394		
Heat Capacity of Basefluid Cp, bf	4179	2347	3281	790	
Density (Kg/m^3)	995.8	1113.2	1073.35	2200	
Particle Cp (J/kgk)				**1200**	
Laminar Flow Condition				**Data Values**	
(Heat flux) q" (w/m^2)		2,500		T_{in} (K)	300
Reynolds (Re)		1,500		ΔT = (T_{out}-T_{in}, K)	5
Nusselt no. (Nu)		48/11			
Friction factor (f)		64/Re			

3. RESULT AND DISCUSSIONS

Assuming the Prasher et al. [53] set condition: C_μ/C_k <4 for effective heat transfer, is examined in Table 2.

Effective Heat Transfer (EHT) condition proposed by Prasher et al. [53] on entropy generation is presented in Table 2 above. The table reveals the variation in the irreversibilties of the different nanofluids within the proposed condition for effective heat transfer. It was observed that the closer the ratio of coefficient of viscosity to thermal conductivity to unity (1), the lower the entropy generated (fluid friction irreversibility, ṠGEN_ff). This implies that entropy generation increases as the said ratio keeps increasing for irreversibility caused by fluid friction, however, irreversibility due to thermal heat remains unaffected all through the ratio variation.

Table 2. Effective Heat Transfer (EHT) on the entropy generation (Prasher et al.) [53]

EHT	Cμ = Ck	Cμ = 2Ck	Cμ = 3Ck	Cμ = 4Ck	Cμ = 5Ck
ṠGEN_ff$_W$	5.16E-07	8.85E-07	1.43E-06	2.19E-06	3.2E-06
ṠGEN_ff$_{EG}$	8.99E-06	1.55E-05	2.51136E-05	3.84804E-05	5.62281E-05
ṠGEN_ff$_{EGW}$	1.8E-06	3.11E-06	5.03E-06	7.7E-06	1.12E-05
ṠGEN_th$_W$	0.000626	0.000626	0.000626	0.000626	0.000626
ṠGEN_th$_{EG}$	0.001458	0.001458	0.001458	0.001458	0.001458
ṠGEN_htf$_{EGW}$	0.000990	0.000990	0.000990	0.000990	0.000990
ṠGEN_tot$_W$	0.000627	0.000627	0.000627	0.000628	0.000629
ṠGEN_tot$_{EG}$	0.001473	0.001483	0.001483	0.001496	0.001514
ṠGEN_tot$_{EGW}$	0.000993	0.000995	0.000995	0.000997	0.001001

3.1 Entropy generation ratio in mini channels

Figure 4 shows that the entropy generation ratio between the graphene nanofluid and the basefluids ($\dot{S}GEN_{,nf}/\dot{S}GEN_{,bf} > 1$) which contradicts the proposed condition for higher efficiency, since there must be low irreversibility and entropy generation [46, 53, 55-58]. This indicates that the suitability of the graphene nanofluids (water (W), ethylene glycol (EG) and ethylene glycol-water blend (EGW_1:1). Hence, the use of nanofluids in microchannels and mini-channels using graphene nanoplatelets with conventional base-fluids under laminar flow regime may need re-consideration for higher efficiencies. Variation of entropy generation ratio with volume fraction in a Micro-channel and Mini-channels are respectively depicted in Figures 4 and 5.

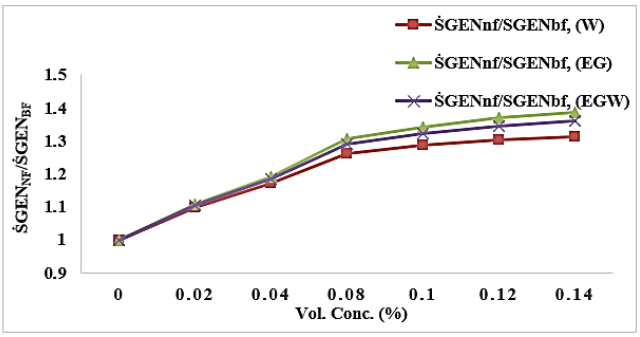

Figure 4. Variation of entropy generation ratio with volume fraction in a micro-channel

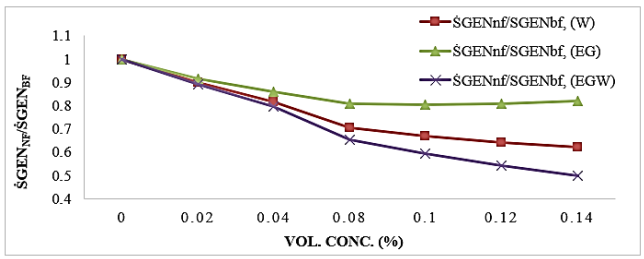

Figure 5. Variation of entropy generation ratio with volume fraction in a mini-channels

Figure 6 shows the variation of entropy generation due to fluid friction ($\dot{S}GEN_{,ff}$) against volume fraction. Observation shows that the $\dot{S}GEN_{,ff}$ of unblended basefluids for ethylene glycol was higher than water (W) and ethylene glycol-water (EGW_1:1) mixture by 50% and 20%, respectively. Same trend was observed with the graphene nanoplatelet (GnP) nanoparticle addition at various volume fraction with the selected basefluids where the least and the highest entropy ratios. This may indicate that the interlayer fluid streams interaction within the basefluids was highly instrumental to the entropy generation in the entire fluid. This means that the interlayer interaction plays a dominant role in the entropy generation of nanoparticles/nanofluids due to fluid friction. It was also observed that entropy generation due to fluid friction increased with increased volume fraction. Meanwhile the entropy generation due to fluid friction for deionized water is lower by 75.6% and higher by 79.9% compared to single ethylene glycol (EG) and the mix of ethylene glycol-water (EGW).

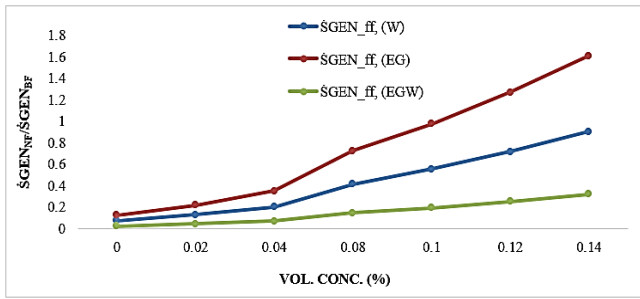

Figure 6. Variation of entropy generation due to fluid friction ($\dot{S}GEN_{,ff}$) in a micro-channel

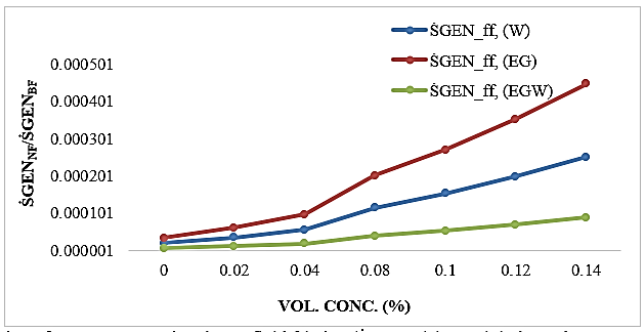

Figure 7. Variation of entropy generation due to fluid friction ($\dot{S}GEN_{,ff}$) in a mini-channel

Figure 7 shows the variation of entropy generation due to fluid friction (ṠGEN, ff) against volume fraction. Unblended (without nanoparticles) ethylene glycol-water (EGW_1:1) basefluid generated the least entropy (ṠGEN, ff). The Sgen, ff of water was higher by 79.9% and lower by 75.6% than EGW and EG, respectively. Here, the Sgen, ff increased with increased volume fraction of GnP nanoparticles. The interlayer fluid stream (IFS) interaction in EGW may be assumed to move relative to each other than single water (W) basefluid or ethylene glycol basefluids. The entropy generated (ṠGEN, ff) in mini-channel was observed to be lower than in micro-channels.

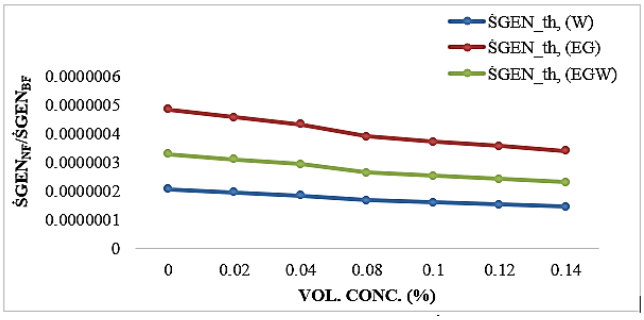

Figure 8. Variation of entropy generation due to fluid friction (ṠGEN, $_{th}$) in a Micro-channel

Figure 8 is the entropy generation due to thermal irreversibility (ṠGEN, th) against volume fraction in a micro-channel. Observation shows that the least ṠGEN, th was with water basefluid. The ṠGEN, th of water was lower by 132.9% and 58.2% than ṠGEN, th of single ethylene glycol (EG) and mix of ethylene glycol-water (EGW). S_{GEN},th of the basefluids decreased with increase in volume fraction. The unblended basefluids (without nanoparticles) showed that the ṠGEN, th was a function of interlayer interaction. This was also observed with basefluids blended with GnP nanoparticle, it may be assumed that the interlayer and interparticle interactions plays dominant role in ṠGEN, th.

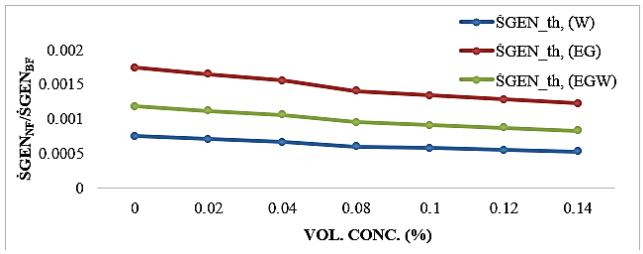

Figure 9. Variation of entropy generation due to fluid friction (ṠGEN, $_{th}$) in a Mini-channel

The entropy generation due to irreversibility in a mini-channel is shown in Figure 9. ṠGEN, th for water basefluid generated the least entropy, followed by the ethylene glycol-water (EGW) basefluid, while the unblended ethylene glycol generated the highest entropy. It is seen that the SGEN, th in all the fluid (nanofluid and basefluids) decreased with increase in volume fraction of nanoparticle. This implies that doping basefluids with GnP nanoparticles reduces the ṠGEN, th when used in micro-channels. This may also imply that both the fluid stream interlayer and the particle to particle (interparticle) interactions move relative to each other for water basefluid/nanofluids.

Figure 10 shows the total entropy generation (ṠGEN, tot) in microchannel. The effect of the part which makes-up the ṠGEN, th resulted in a least magnitude of ṠGEN, tot when a mix of ethylene glycol-water is used compared to single water (W) or ethylene glycol with and without GnP nanoparticle. Overall, the ṠGEN, tot using water basefluid was lower by 75.6% and higher by 64.8% than single ethylene glycol and water (EGW), respectively. This implies that EGW is more suitable as basefluid in micro-channels since they generated the least entropy. Generally, result shows that total S_{GEN}, tot increased with increase in volume fraction of GnP.

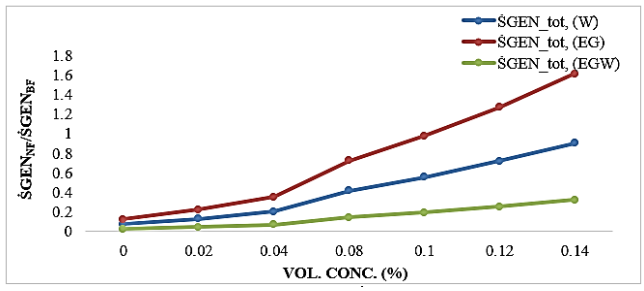

Figure 10. Variation of total entropy generation (ṠGEN, $_{tot.}$) in a Micro-channel

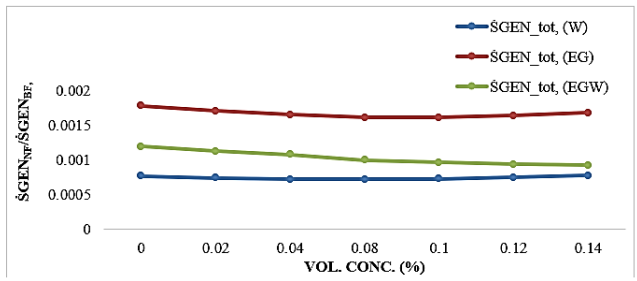

Figure 11. Variation of total entropy generation (ṠGEN, $_{tot.}$) in a Mini-channel

Figure 11 is the total entropy generation (ṠGEN, tot) in a minichannel. The least entropy was generated using single water basefluid and then mixture of ethylene glycol-water (EGW), while the highest total entropy was obtained using single ethylene glycol basefluid. Observation shows that at 0.08 volume fraction, GnP nanoparticle blend generated the least ṠGEN, tot for the single basefluid. This implies that single nanofluid is more suitable in mini-channels. The ṠGEN, tot using water (W) basefluid is lower by 123.7% and 38.4% compared to single ethylene glycol (EG) and mixture of ethylene glycol-water (EGW).

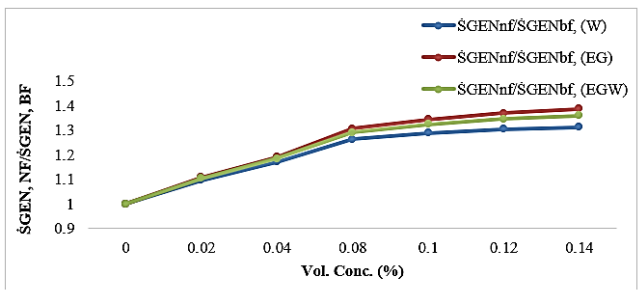

Figure 12. Variation of entropy generation ratio (ṠGEN.) in a Mini-channel

Figure 12 shows the entropy generation ratio (ṠGEN,nf/ṠGEN,bf) in micro-channel. Here, the ṠGEN,nf/ṠGEN,bf increased beyond unity. Addition of nanoparticles only increased the S_{GEN},nf/S_{GEN},bf and it indicates that the nanofluids are not suitable for use in micro-channels, though water basefluid had the least ṠGEN,nf/ṠGEN,bf.

Entropy generation ratio (ṠGEN,nf/ṠGEN,bf (3mm) in a mini-channel is shown in Figure 13. Result shows that the ṠGEN,nf/ ṠGEN,bf of unblended basefluid was at unity, which decreased as GnP nanoparticle volume fraction was

increased. This shows the influence of thermal properties (ρnf and Knf) of the nanoparticles on the basefluid, wherein, there is an improvement in the ṠGEN,nf/ṠGEN,bf by decreasing as the volume fraction increases. It means the use of nanofluid is suitable for lowering ṠGEN,nf/ṠGEN,bf in mini-channels. The ṠGEN,nf/ṠGEN,bf decreased with increased volume fraction of GnP nanofluid, while the mixture of ethylene glycol-water (EGW) had the least ṠGEN,nf/ ṠGEN,bf, hence, more suitable in mini-channel.

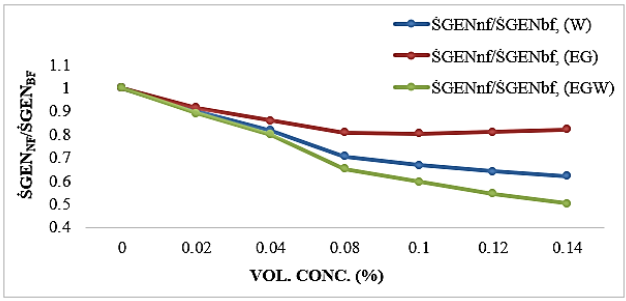

Figure 13. Variation of (ṠGEN,nf/ṠGEN,bf) in a mini-channel

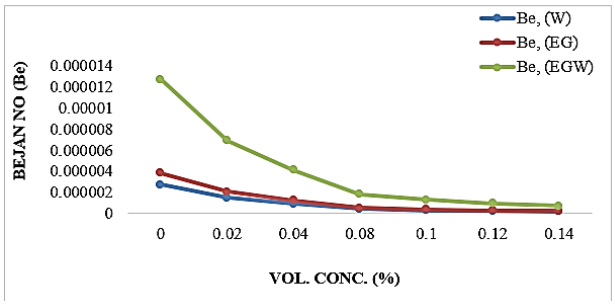

Figure 14. Variation of Bejan number (Be) in a micro-channel

Bejan number (Be) of the microchannel is shown in Figure 14 as a function of volume fraction. The low Be is an indication that the effect of thermal irreversibility (ṠGEN, th) is less dominant compared to entropy generation due to fluid friction (ṠGEN, ff). It was also observed that the Be of water based basefluid/nanofluid was lower by 36.8% and 358.9% than single ethylene glycol and mixture of ethylene glycol-water (EGW), respectively.

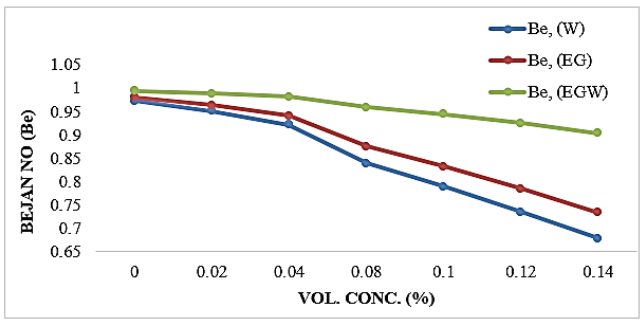

Figure 15. Variation of Bejan number (Be) in a mini-channel

Figure 15 shows the Bejan number (Be) as a function of volume fraction in a mini-channel. The effect of thermal irreversibility (ṠGEN, th) is dominant in the result for all the basefluids/nanofluids as the result for volume fraction were between 0.6 and 1. Meanwhile, ṠGEN, th is more dominant in the mixture of ethylene glycol-water (EGW) than the single basefluids nanofluids. This may be as a result of the heat generated during stream/particle interaction. The Be number of water based basefluids/nanofluids is lower by 3.8% and 13.8% than the single ethylene glycol and mixture of ethylene glycol-water (EGW) The Be number decreased with increase in volume fraction of GnP nanoparticle.

4. CONCLUSION

Entropy generation of GnP blended in different basefluids under laminar flow condition for micro and mini-channels using conductivity and viscosity models was investigated in this study. GnP is not recommended for utilization in micro-channels (ṠGEN, nf/ ṠGEN, bf >1) and its entropy generation ratio increases as its volume concentration increases. Meanwhile, in mini-channels, entropy generation ratio decreases as volume concentration of GnP increases and ṠGEN,nf/ṠGEN, bf <1, making its utilization beneficial. Hence in micro-channels,

- Total entropy generation, ṠGEN, tot for GnP-water nanofluid was lower by 75.6% and higher by 64.8% compared to EG and EGW, respectively.
- Bejan number for water (Be_w) was lower by 36.8% and 358.9% compared to EG and EGW and in mini-channels,
- Total entropy generation, ṠGEN, tot for GnP-water nanofluid was observed to be lower compared to EG and EGW by 123.7% and 38.4%, respectively.
- Bejan number for water (Be_w) was lower by 3.8% and 13.8% when compared to EG and EGW nanofluids.

Generally, the result from the study indicates that GnP and water nanofluid generates the least entropy in mini-channels and can utilized in various applications including automotive cooling.

REFERENCES

[1] Jain, S., Gupta, P. (2019). Entropy generation analysis of carbon nanotubes nanofluid 3D flow along a nonlinear inclined stretching sheet through porous media. International Journal of Heat and Technology, 37(1): 131-138. https://doi.org/10.18280/ijht.370116

[2] Vyas, P., Khan, S. (2021). Dual entropy regime in channel flow subjected to temperature dependent convection mechanism. International Journal of Heat and Technology, 39(2): 424-432. https://doi.org/10.18280/ijht.390211

[3] Bhat, P., Katte, S.S. (2020). Entropy analysis of a simple rectangular radiating fin for space applications. International Journal of Heat and Technology, 38(3): 708-714. https://doi.org/10.18280/ijht.380315

[4] Reddy, S.R.R., Reddy, P.B.A. (2021). Entropy generation analysis on MHD flow with a binary mixture of ethylene glycol and water based silver-graphene hybrid nanoparticles in automotive cooling systems. International Journal of Heat and Technology, 39(6): 1781-1790. https://doi.org/10.18280/ijht.390611

[5] Kazeem, R.A., Amakor, J.U., Ikumapayi, O.M., Afolalu, S.A., Oke, W.A. (2022). Modelling the effect of temperature on power generation at a Nigerian agricultural institute. Mathematical Modelling of Engineering Problems, 9(3): 645-654. https://doi.org/10.18280/mmep.090311
[6] Afolalu, S.A., Ikumapayi, O.M., Ogundipe, A.T., Yusuf, O.O., Oloyede. O.R. (2021). Development of nanolubricant using aloe vera plant to enhance the thermal performance of a domestic refrigeration system. International Journal of Heat and Technology, 39(6): 1904-1908. https://doi.org/10.18280/ijht.390626
[7] Cao, H.Y., Guo, Z.X., Xiang, H., Gong, X.G. (2012). Layer and size dependence of thermal conductivity in multilayer graphene nanoribbons. Phys. Lett. A., 376(4): 525-528. https://doi.org/10.1016/j.physleta.2011.11.016
[8] Ansari, R., Motevalli, B., Montazeri, A., Ajori, S. (2011). Fracture analysis of monolayer graphene sheets with double vacancy defects via MD simulation. Solid State Commun., 151(17): 1141-1146. https://doi.org/10.1016/j.ssc.2011.05.021
[9] Bhuyan, M.S.A., Uddin, M.N., Islam, M.M., Bipasha, F.A., Hossain, S.S. (2016). Synthesis of graphene. Int Nano Lett., 6: 65-83. https://doi.org/10.1007/s40089-015-0176-1
[10] Prezhdo, O.V., Kamat, P.V., Schatz, G.C. (2011). Virtual issue: Graphene and functionalized graphene. J. Phys. Chem. C., 115(8): 3195-3197. https://doi.org/10.1021/jp200538f
[11] Wu, Y.H., Yu, T., Shen, Z.X. (2010). Two-dimensional carbon nanostructures: FUNDAMENTAL properties, synthesis, characterization, and potential applications. J. Appl. Phys., 108(7): 071301. https://doi.org/10.1063/1.3460809
[12] Vadukumpully, S., Paul, J., Valiyaveettil, S. (2009). Cationic surfactant mediated exfoliation of graphite into graphene flakes. Carbon, 47(14): 3288-3294. https://doi.org/10.1016/j.carbon.2009.07.049
[13] Meng, Z., Wu, D., Wang, L., Zhu, H., Li, Q. (2012). Carbon nanotube glycol nanofluids: Photo-thermal properties, thermal conductivities and rheological behavior. Particuology, 10(5): 614-618. https://doi.org/10.1016/j.partic.2012.04.001
[14] Halelfadl, S., Estellé, P., Aladag, B., Doner, N., Maré, T. (2013). Viscosity of carbon nanotubeswater-based nanofluids: Influence of concentration and temperature. Int. J. Therm. Sci., 71: 111-117. https://doi.org/10.1016/j.ijthermalsci.2013.04.013
[15] Mahbubul, I., Khan, M.M.A., Ibrahim, N.I., Ali, H.M., Al-Sulaiman, F.A., Saidur, R. (2018). Carbon nanotube nanofluid in enhancing the efficiency of evacuated tube solar collector. Renew. Energy, 121: 36-44. https://doi.org/10.1016/j.renene.2018.01.006
[16] Chen, L., Xie, H., Li, Y., Yu, W. (2008). Nanofluids containing carbon nanotubes treated by mechanochemical reaction. Thermochim. Acta, 477(1-2): 21-24. https://doi.org/10.1016/j.tca.2008.08.001
[17] Vryzas, Z., Kelessidis, V.C. (2017). Nano based drilling fluids: A review. Energies, 10(4): 540. https://doi.org/10.3390/en10040540
[18] Ismail, A., Aftab, A., Ibupoto, Z., Zolkifile, N. (2016). The novel approach for the enhancement of rheological properties of water-based drilling fluids by using multi-walled carbon nanotube, nanosilica and glass beads. J. Pet. Sci. Eng., 139: 264-275. https://doi.org/10.1016/j.petrol.2016.01.036
[19] Balandin, A.A., Ghosh, S., Bao, W., Calizo, I., Teweldebrhan, D., Miao, F., Lau, C.N. (2008). Superior thermal conductivity of single-layer graphene. Nano Lett., 8(3): 902-907. https://doi.org/10.1021/nl0731872
[20] Arshad, A., Jabbal, M., Yan, Y., Reay, D.A. (2019). Review on graphene based nanofluids: Preparation, characterization and applications. J. Mol. Liq., 279: 444-484. https://doi.org/10.1016/j.molliq.2019.01.153
[21] Hamze, S., Cabaleiro, D., Estellé, P. (2021). Graphene-based nanofluids: A comprehensive review about rheological behavior and dynamic viscosity. J. Mol. Liq., 325: 115207. https://doi.org/10.1016/j.molliq.2020.115207
[22] Wang, Y., Al-Saaidi, H.A.I., Kong, M., Alvarado, J.L. (2018). Thermophysical performance of graphene based aqueous nanofluids. Int. J. Heat Mass Transf., 119: 408-417. https://doi.org/10.1016/j.ijheatmasstransfer.2017.11.019
[23] Kole, M., Dey, T.K. (2013). Investigation of thermal conductivity, viscosity, and electrical conductivity of graphene based nanofluids. J. Appl. Phys., 113(8): 084307. https://doi.org/10.1063/1.4793581
[24] Moghaddam, M.B., Goharshadi, E.K., Entezari, M.H., Nancarrow, P. (2013). Preparation, characterization, and rheological properties of graphene–glycerol nanofluids. Chem. Eng. J., 231: 365-372. https://doi.org/10.1016/j.cej.2013.07.006
[25] Kazemi, I., Sefid, M., Afrand, M. (2020). A novel comparative experimental study on rheological behavior of mono & hybrid nanofluids concerned graphene and silica nano-powders: Characterization, stability and viscosity measurements. Powder Technol., 366: 216-229. https://doi.org/10.1016/j.powtec.2020.02.010
[26] Lee, S.H., Lee, D.H., Lee, W.J., Kim, S.O. (2011). Tailored assembly of carbon nanotubes and graphene. Adv. Funct. Mater., 21: 1338-1354. https://doi.org/10.1002/adfm.201002048
[27] Wu, Y.H., Yu, T., Shen, Z.X. (2010). Two-dimensional carbon nanostructures: Fundamental properties, synthesis, characterization, and potential applications. J. Appl. Phys., 108(7): 071301. https://doi.org/10.1063/1.3460809
[28] Chae, H.K., Siberio-Pérez, D.Y., Kim, J., Go, Y., Eddaoudi, M., Matzger, A.J., O'Keeffe, M., Yaghi, O.M. (2004). A route to high surface area, porosity and inclusion of large molecules in crystals. Nature, 427: 523-527. https://doi.org/10.1038/nature02311
[29] Liu, Y., Xie, B., Zhang, Z., Zheng, Q., Xu, Z. (2012). Mechanical properties of graphene papers. J. Mech. Phys. Solids, 60(4): 591-605. https://doi.org/10.1016/j.jmps.2012.01.002
[30] Chu, K., Li, W.S., Dong, H.F., Tang, F.L. (2012). Modeling the thermal conductivity of graphene nanoplatelets reinforced composites, europhys. Lett., 100(3): 36001. https://doi.org/10.1209/0295-5075/100/36001
[31] Novoselov, K.S., Fal'ko, V.I., Colombo, L., Gellert, P.R., Schwab, M.G., Kim, K. (2012). A roadmap for graphene. Nature, 490(7419): 192-200. https://doi.org/10.1038/nature11458
[32] Monireh, B.V., Ali, A.S., Amir, A.P., Leila, M. (2018). Physical adsorption of horseradish peroxidase on

reduced graphene oxide nanosheets functionalized by amine: A good system for biodegradation of high phenol concentration in wastewater. International Journal of Environmental Research, 12(1): 45-57. https://doi.org/10.1007/s41742-018-0067-1

[33] Selvama, C., Mohan Lal, D., Harish, S. (2016). Thermal conductivity enhancement of ethylene glycol and water with graphene nanoplatelets. Thermochimica Acta, 642: 32-38. https://doi.org/10.1016/j.tca.2016.09.002

[34] Esfahani, M.R., Nunna, M.R., Languri, E.M., Cunningham, G. (2018). Experimental study on heat transfer and pressure drop of in-house synthesized graphene oxide nanofluids. Heat Transfer Engineering, 40(8): 1-42. https://doi.org/10.1080/01457632.2018.1497001

[35] Bahaya, B., Johnson, D.W., Yavuzturk, C.C. (2018). On the effect of graphene nanoplatelets on water–graphene nanofluid thermal conductivity, viscosity, and heat transfer under laminar external flow conditions. Journal of Heat Transfer, 140(6): 1-4. https://doi.org/10.1115/1.4038835

[36] Bejan, A. (1980). Second law analysis in heat transfer. Energy, 5(8-9): 720-732. https://doi.org/10.1016/0360-5442(80)90091-2

[37] Bejan, A. (1978). General criterion for rating heat-exchanger performance. Inter. J. Heat Mass Transfer, 21(5): 655-658. https://doi.org/10.1016/0017-9310(78)90064-9

[38] Cengel, Y.A., Boles, M.A. (2006). Thermodynamics: An Engineering Approach. McGraw-Hill Higher Education: New York, NY, USA.

[39] Carnahan, W., Ford, K.W., Prosperetti, A., Rochlin, G.I., Rosenfeld, A.H., Ross, M.H., Rothberg, J.E., Seidel, G.M., Socolow, R.H. (2013). Efficient use of energy: A physics perspective. New York: Am. Phys. Society: January. Study Report 1975, 399: 242-773. Entropy, 15, 155.

[40] Bouabid, M., Magherbi, M., Hidouri, N., Brahim, A.B. (2011). Entropy generation at natural convection in an inclined rectangular cavity. Entropy, 13(5): 1020-1033. https://doi.org/10.3390/e13051020

[41] Bejan, A. (1982). Chapter 5. In Entropy Generation through Heat and Fluid Flow. John Willy and Sons: NY, USA, 1982.

[42] Bejan, A. (1979). A Study of entropy generation in fundamental convective heat transfer. J. Heat Trans., 101(4): 718-725. https://doi.org/10.1115/1.3451063

[43] Sadeghinezhad, E., Mehrali, M., Saidur, R. (2016). A comprehensive review on graphene nanofluids: recent research, development and applications. Energy Convers Manag., 111: 466-487. https://doi.org/10.1016/j.enconman.2016.01.004

[44] Yuan, Y., Zhang, N., Li, T. (2016). Thermal performance enhancement of palmitic-stearic acid by adding graphene nanoplatelets and expanded graphite for thermal energy storage: A comparative study. Energy, 97: 488-497. https://doi.org/10.1016/j.energy.2015.12.115

[45] Hadadian, M., Goharshadi, E.K., Youssefi, A. (2014). Electrical conductivity, thermal conductivity, and rheological properties of graphene oxide-based nanofluids. J Nanoparticle Res., 16(12): 1-17. https://doi.org/10.1007/s11051-014-2788-1

[46] Singh, P.K., Anoop, K., Sundararajan, T., Das, S.K. (2010). Entropy generation due to flow and heat transfer in nanofluids. Inter. J. Heat Mass Trans., 53(21-22): 4757-4767. https://doi.org/10.1016/j.ijheatmasstransfer.2010.06.016

[47] Einstein, A. (1911). Berichtigung zu meiner arbeit: Eine neue bestimmung der moleküldimensionen. Ann. Phys., 14: 591-592.

[48] Hamilton, R., Crosser, O. (1962). Thermal conductivityof heterogeneous two-component systems. Ind. Engin. Chem. Funda., 1(3): 187-191. https://doi.org/10.1021/i160003a005

[49] Nan, C.W., Birringer, R., Clarke, D.R., Gleiter, H. (1997). Effective thermal conductivity of particulate composites with interfacial thermal resistance. J. Appl. Phys., 81: 6692-6699. https://doi.org/10.1063/1.365209

[50] Ghozatloo, A., Rashidi, A., Shariaty-Niassar, M. (2014). Convective heat transfer enhancement of graphene nanofluids in shell and tube heat exchanger. Exp. Therm. Fluid Sci., 53: 136-141. https://doi.org/10.1016/j.expthermflusci.2013.11.018

[51] Bing, N., Yang, J., Zhang, W., Yu, Y., Wang, L., Xie, H. (2020). 3D graphene nanofluids with high photothermal conversion and thermal transportation properties. Sustain. Energy Fuels, 4(3): 1208-1215. https://doi.org/10.1039/C9SE00866G

[52] Wang, Z., Wu, Z., Han, F., Wadsö, L., Sundén, B. (2018). Experimental comparative evaluation of a graphene nanofluid coolant in miniature plate heat exchanger. Int. J. Therm. Sci. 130: 148-156. https://doi.org/10.1016/j.ijthermalsci.2018.04.021

[53] Dresselhaus, M.S., Rao, A.M., Dresselhaus, G. (2004). Encyclopedia of Nano Science and Nanotechnology, 307-338.

[54] Zheng, R., Gao, J. Wang, J., Feng, S.P., Ohtani, H., Wang, J., Chen, G. (2011). Thermal percolation in stable graphite suspensions. Nano Lett., 12(1): 188-192. https://doi.org/10.1021/nl203276y

[55] Yu, W., Xie, H., Wang, X., Wang, X. (2011). Significant thermal conductivity enhancement for nanofluids containing graphene nanoplatelets. Phys. Lett. A, 375(10): 1323-1328. https://doi.org/10.1016/j.physleta.2011.01.040

[56] Hajjar, Z., Rashidi, A.M., Ghozatloo, A. (2014). Enhanced thermal conductivities of graphene oxide nanofluids. Int. Commun. Heat Mass Transf., 57: 128-131. https://doi.org/10.1016/j.icheatmasstransfer.2014.07.018

[57] Kamatchi, R., Venkatachalapathy, S., Srinivas, A.B. (2015). Synthesis stability, transport properties, and surface wettability of reduced grapheneoxide/water nanofluids. Int. J. Therm. Sci., 97: 17-25. https://doi.org/10.1016/j.ijthermalsci.2015.06.011

[58] Prasher, R., Song, D., Wang, J., Phelan, P. (2006). Measurements of nanofluid viscosity and its implications for thermal applications. Appl. Phys. Lett., 89(13): 133108-133103. https://doi.org/10.1063/1.2356113

NOMENCLATURE

ṠGEN	Entropy generation rate, W/m.k
Ck	Coefficient of thermal conductivity
Cμ	Coefficient of viscosity
Be	Bejan number
Φ	Volume fraction of particle
k	Thermal conductivity
ρ	Density
T	Temperature
GnP	Graphene Nanoplatelet
q"	Unit length heat flux, W/m
Re	Reynolds number
D	Tube diameter, m
f	friction factor
Cp	Specific heat, J/kg.k
μ	viscosity, kg. $m^{-1}.s^{-1}$
m	mass flowrate
n	Shape constant

Subscripts

ff	Fluid friction
th	thermal heat
tot	Total
bf	Basefluid
nf	Nanofluid
W	Water
EG	Ethylene glycol
EGW	Ethylene glycol-water